Molecular insight into inhibitory performance of CTAB surfactant for montmorillonite swelling; implications for drilling fluid design

DOI:
10.1016/j.geoen.2023.212399

Document Version
Accepted author manuscript

Molecular Insight into Inhibitory Performance of CTAB Surfactant for Montmorillonite Swelling; Implications for Drilling Fluid Design

Mehdi Karimi[a], Mehdi Ghasemi[b*], Masoud Babaei[b], Khalil Shahbazi[a*],

[a] *Department of Petroleum Engineering, Ahwaz Faculty of Petroleum Engineering, Petroleum University of Technology, Ahwaz 63134, Iran*

[b] *Department of Chemical Engineering, The University of Manchester, Manchester, UK.*

** Corresponding authors:*

E-mail addresses: Mehdi.ghasemi@postgrad.manchester.ac.uk, meghasemi96@gmail.com (M. Ghasemi), shahbazi@put.ac.ir (K. Shahbazi)

Graphical Abstract

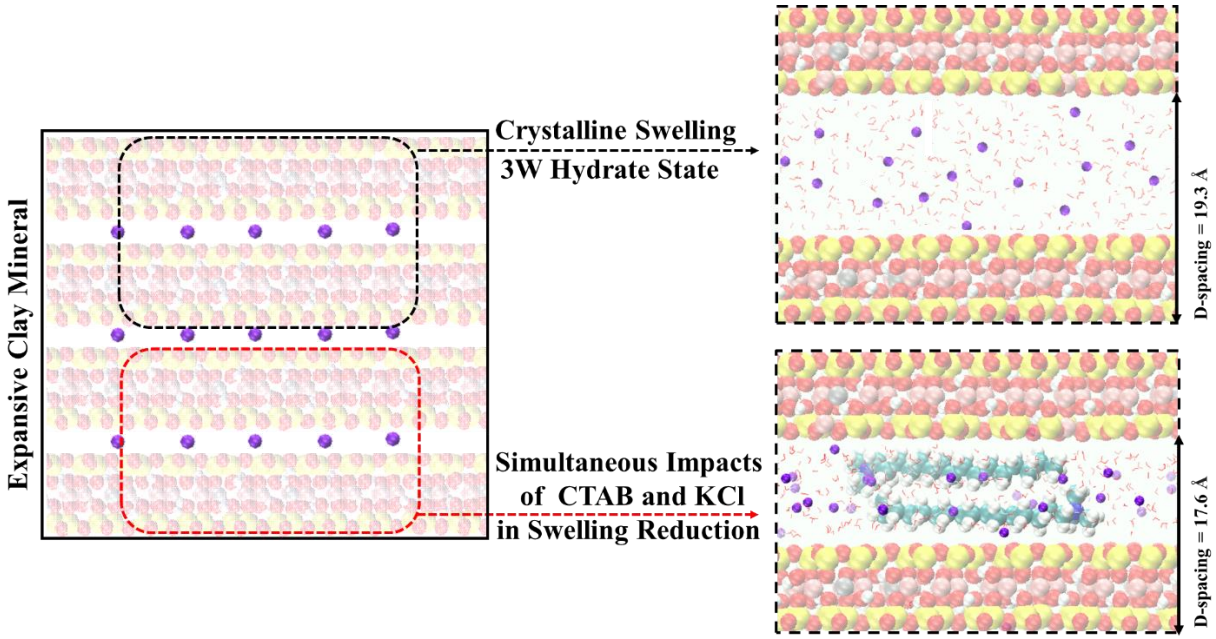

Abstract

The swelling behavior of expansive clay minerals, specifically montmorillonite (MMT), can impose severe challenges (e.g., hole instability) during subsurface drilling when the inhibitory properties of drilling fluid are not appropriately optimized. In this research work, the molecular dynamics (MD) were employed to quantitatively evaluate the inhibitory performance of cetyltrimethylammonium bromide (CTAB) in retarding the transition state between crystalline and osmotic swelling of sodium montmorillonite (Na-MMT). The combined impacts of CTAB and KCl were assessed, and inhibition mechanisms were also elucidated. Comprehensive trajectory-based analyses showed that an addition of 10 g/L CTAB into the Na-MMT interlayer reduces the *d*-spacing by 5.18% from 19.3 Å to 18.3 Å, through cation-exchange, wettability alteration, and surface charge compensation mechanisms. The parallel orientation of CTA^+ cations to the clay surface, forming monolayer and bilayer structures, assists in bringing the clay layers closer together. The assessment of the combined impacts of inhibitors revealed that, despite the Na^+ cations having a higher hydration enthalpy compared to K^+ cations, the higher ratio of K^+/Na^+ diminishes the performance of the combined CTAB and KCl. Our results showed that the addition of KCl up to 8 wt% into the interlayer improves the inhibitory performance of 10 g/L CTAB by further decreasing the *d*-spacing to 17.6 Å.

Keywords: Na-Montmorillonite Swelling, CTAB surfactant, Inhibition mechanisms, Drilling Fluids, Molecular dynamics (MD) simulation

1. Introduction

Among the entire spectrum of categories of clay minerals, a 2:1 clay mineral named montmorillonite (MMT), which frequently exists in geological formation, has the most swelling potential (Gholami et al., 2018). MMT is composed of one octahedral sheet (O-sheet) placed between two tetrahedral sheets (T-sheets) (Skipper et al., 1995). The TOT layers of MMT have negative charge originating from isomorphic substitutions of Mg^{2+} for Al^{3+} in O-sheets and Al^{3+} for Si^{4+} in T-sheets, and these negative charges are balanced by counterions (Chang et al., 1995). The swelling characteristics of MMT are basically described through two distinct patterns: crystalline swelling and osmotic swelling (Norrish, 1954). The stepwise adsorption of water molecules from one to three hydration states causes the crystalline swelling, while the osmotic swelling occurs due to the higher water uptake into the interlayers causing expansion up to 120 Å (Greathouse et al., 2016). Clay minerals susceptible to water sensitivity may undergo crystalline swelling. However, it is essential to postpone the transition of MMT swelling from the crystalline phase to the osmotic phase, due to its high swelling capability.

The drilling process for underground reservoirs commonly employs remarkably effective water-based drilling fluids (WBDFs) because of their environmentally conscious nature and cost-effectiveness (Mahto and Sharma, 2004; Zeynali, 2012). Nonetheless, the drilling of shale formations abundant in clay minerals frequently gives rise to challenges about the stability of the wellbore (Ghasemi et al., 2019; Zhong et al., 2015). This arises due to the existence of expansive clay minerals, which are sensitive to water, can interact with the aqueous phase of WBDFs, resulting in swelling and a subsequent reduction in compressive strength, thus imposing wellbore instability (Chenevert, 1970).

A wide range of inhibitors with varying physical and chemical properties have been developed for WBDFs to address challenges associated with clay swelling (Muhammed et al., 2021). Among the most studied inhibitors are salts (Li et al., 2019; Zhang et al., 2022), polymers (Abbas et al., 2021; Ahmed et al., 2019), amines (Barati et al., 2017; Suter et al., 2011), silicates (Murtaza et al., 2020), nanoparticles (Saleh and Ibrahim, 2019), ionic liquids (Ahmed Khan et al., 2020), deep eutectic solvents (Jia et al., 2019), etc. Each additive can use either a single mechanism or a combination of inhibition mechanisms, namely wettability change, cation exchange, pore plugging, osmotic backflow, encapsulation, and filtrate viscosity increment (Suter et al., 2011).

Surfactants, particularly non-ionic and cationic types, have emerged as promising inhibitors for mitigating MMT swelling as a result of their robust interactions with the negatively charged clay layers (Ahmad et al., 2023). These types of surfactants have attracted significant attention for their superior inhibitive performance. Numerous experimental investigations have been undertaken to evaluate the performance of surfactants as inhibitors for mitigating clay swelling (Quintero, 2002). Among these surfactants, cetyltrimethylammonium bromide (CTAB) has received significant attention from researchers. For example, Moslemizadeh et al. (Moslemizadeh et al., 2016) found that CTAB exhibited superior performance compared to deionized water in terms of reducing water adsorption on the clay surface and maintaining desired properties of WBDFs at higher MMT loading. They proposed cation exchange as the primary inhibition mechanism of CTAB. Similarly, Yue et al. (Yue et al., 2018) carried out research where they noted a rise in the contact angle of a modified shale surface upon treatment with CTAB, indicating the positive impact of CTAB in mitigating wellbore instability. They proposed that the inhibition mechanism of CTAB involves ionic bonding, where the hydrated CTA^+ cation interacts with the clay surface and orients its hydrophobic tail towards the aqueous phase. Bi et al. (Bi et al., 1999) also evaluated the effect of

CTAB on clay swelling and observed a 4% reduction in swelling rate. As a representative of cationic surfactants, CTAB has demonstrated potential as a clay swelling inhibitor. However, a comprehensive understanding of its mechanism in retarding the transition state from crystalline phase to osmotic swelling remains absent. This knowledge gap holds particular significance in subsurface drilling, where osmotic swelling can give rise to formidable challenges.

In the past few years, the utilization of molecular dynamics (MD) simulations has become increasingly prevalent, facilitated by the advancement of high-performance computing systems (Omrani et al., 2023; Tazikeh et al., 2021). MD simulations offer a valuable tool for obtaining detailed insights into molecular structures, particle interactions, and the dynamic behavior of systems last stage of crystalline (Frenkel et al., 1996; Ghamartale et al., 2023; Ghamartale et al., 2020; Hensen et al., 2001).

Numerous studies have employed MD simulations to explore the swelling characteristics of various clay minerals, considering different influential factors based on the structure (Chang et al., 1998b; Dazas et al., 2015; Du et al., 2020; Jia et al., 2019; Narayanan Nair et al., 2021; Rahromostaqim and Sahimi, 2018). Additionally, several studies have explored the effects of inorganic salts (Bourg and Sposito, 2011; Camara et al., 2017; Jiafang et al., 2014), polymers (Suter et al., 2011; Xie et al., 2022; Xu et al., 2023), and nanoparticles (de Lara et al., 2017) on clay swelling. Nevertheless, no study has specifically focused on the quantitative and mechanistic evaluation of surfactants as clay swelling inhibitors, in conjunction with KCl, the most commonly used inhibitor in the industry, from a molecular insight perspective.

In this research work, the inhibitory performance of CTAB as a clay swelling inhibitor was investigated from an atomic perspective. Our primary objective was to scrutinize the extent to which the coaction of CTAB and KCl can impede the transition state between crystalline swelling

and osmotic swelling. For the simulation, we specifically considered the last stage of crystalline swelling, where three water (3W) hydration states are formed. Trajectory-based analyses, namely interlayer space (*d*-spacing), density profile, radial distribution functions (RDFs), surface charge density, and diffusion coefficient were employed to elucidate the inhibitory mechanisms of studied cases. In summary, the followings are the key attributes of this study to the literature:

- Elucidating the governing inhibition mechanisms of CTAB, as a representative of a cationic surfactant, from atomic perspective: reduction in clay swelling by CTAB is not achieved through a sole mechanism, but through the simultaneous impacts of several mechanisms, namely cation exchange, wettability alteration, and surface charge compensation.
- Revealing the role of the structural arrangement of CTA^+ cations in inhibition mechanisms: the structural arrangement of CTA^+ cations in the form of monolayer and bilayer structures, oriented in parallel with the clay slab, assists in bringing the layers closer together.
- Providing new insight into the coactions of inhibitors with different natures: CTAB and KCl do not necessarily improve the inhibitory performance, as it depends on the KCl concentration for achieving the optimum inhibitory performance of the combined inhibitors.

In the subsequent sections of the paper, we will provide an explanation of the system preparation and simulation procedures in Section 2. The interpretation of the conducted analyses will be presented in Section 3. Section 4 elaborates on the significance of the topic in subsurface drilling, followed by the presentation of our conclusions in Section 5.

2. Methodology

2.1. Model preparation

The Na-MMT structure was constructed based on the pyrophyllite structure with $Na_{0.75}[Al_{0.25}Si_{7.75}][Al_{3.5}Mg_{0.5}]O_{20}(OH)_4$ chemical formula (Lee and Guggenheim, 1981). The supercell with the size of 12×10 was obtained by converting the unit-cell. Isomorphic substitutions of Al^{+3} by Mg^{+2} atoms and Si^{+4} by Al^{3+} atoms were randomly introduced in the O-sheet and T-sheets, respectively, to replicate the chemical structure of MMT (Ghasemi and Sharifi, 2021). The dimensions of the simulation box in various directions are as $x: 6.192\,\text{nm}$, $y: 8.96\,\text{nm}$, and $z: 3.86\,\text{nm}$. Two layers of MMT were stacked, and Na^+ counterions were randomly introduced into the middle of clay slabs to neutralize the negative charge present within them. Since the focus of the study was the 3W hydrate state, 15 molecules/unit-cell of water were inserted in the interlayers of MMT (Chang et al., 1998a). For an accurate representation of concentration, CTAB concentrations of 6 g/L and 10 g/L were chosen based on the optimal values introduced by Moslemizadeh et al (Moslemizadeh et al., 2016). Additionally, to examine the combined impacts of CTAB and KCl, three standard concentrations of 5, 8, and 12 wt% were chosen based on the following reference (Shi et al., 2019). The simulated cases and number of each ion are shown in **Table 1**. Note that the concentrations selected for the simulation are limited to inside the clay minerals, and they are not necessarily the same as the concentrations outside the clay layers.

Table 1. The number of each component in various simulation systems. Note that the number of water molecules is constant for all cases.

Case	System	CTA^+	Br^-	Na^+	K^+	Cl^-
1	Na-MMT + Water	–	–	180	–	–
2	Na-MMT + Water + CTAB 6 g/L	4	4	180	–	–
3	Na-MMT + Water + CTAB 6 g/L + KCl 5 wt%	4	4	180	45	45
4	Na-MMT + Water + CTAB 6 g/L + KCl 8 wt%	4	4	180	72	72
5	Na-MMT + Water + CTAB 6 g/L + KCl 12 wt%	4	4	180	108	108
6	Na-MMT + Water + CTAB 10 g/L	6	6	180	–	–

7	Na-MMT + Water + CTAB 10 g/L + KCl 5 wt%	6	6	180	45	45
8	Na-MMT + Water + CTAB 10 g/L + KCl 8 wt%	6	6	180	72	72
9	Na-MMT + Water + CTAB 10 g/L + KCl 12 wt%	6	6	180	108	108

2.2. Potential models

For modeling the clay mineral slab, the accurate and well-known force field of CLAYFF was employed (Cygan et al., 2021; Cygan et al., 2004). This force field predominantly employs Lennard-Jones and Coulomb potentials to model nonbonded interactions within the clay slab, while bonded interactions are utilized to accurately simulate the hydroxyl structure (Ghasemi et al., 2022). As for the CTAB surfactant, we utilized the CHARMM36 (Bjelkmar et al., 2010; Vanommeslaeghe et al., 2010), which has been primarily developed for organic molecules (Yazhgur et al., 2018). The compatibility between CHARMM36 and CLAYFF force fields has been previously confirmed in the literature (Ghasemi and Shafiei, 2022; Wright and Walsh, 2012). Moreover, we employed the TIP3P water model, selected for its compatibility with the CLAYFF and CHARMM36 force fields (Wright and Walsh, 2012). To describe Van der Waals interactions between atoms from distinct molecules, we incorporated the Lorentz-Berthelot mixing rules. All the potential parameters used to define the intermolecular interactions of the molecules were tabulated in Supporting Information (SI), section (A).

2.3. Simulation details

MD simulations were conducted utilizing GROMACS software (Version 2022) (Van Der Spoel et al., 2005), and the visualization of systems was accomplished using the VMD software (Humphrey et al., 1996). The simulation protocol consisted of several steps. Initially, energy minimization was conducted with 100,000 steps. Following energy minimization, MD simulations lasting 2 ns were performed in the *NPT* ensemble with 1 fs time step to attain an equilibrated *d*-spacing. The temperature was maintained at 298 K, and the pressure was set to 1 bar. Reaching an equilibrium

state was confirmed by root-mean-square deviation (*RMSD*) analysis, as detailed in SI, section (B). Subsequently, equilibrated configurations were employed to perform 30 ns MD simulations in *NVT* ensemble. Temperature was controlled using a V-rescale thermostat (Bussi et al., 2007), while pressure was regulated through an isotropic Parrinello-Rahman barostat (Nosé and Klein, 1983). A non-bonded interaction calculation was conducted using a cutoff value of 1.20 nm. Periodic boundary conditions (PBCs) were incorporated in all dimensions. Data sampling for subsequent analyses was done over the last 5 ns of the production run, where the system reached an equilibrium state. The molecular structure of CTAB and initial configuration of the simulation system are depicted in **Figure 1**.

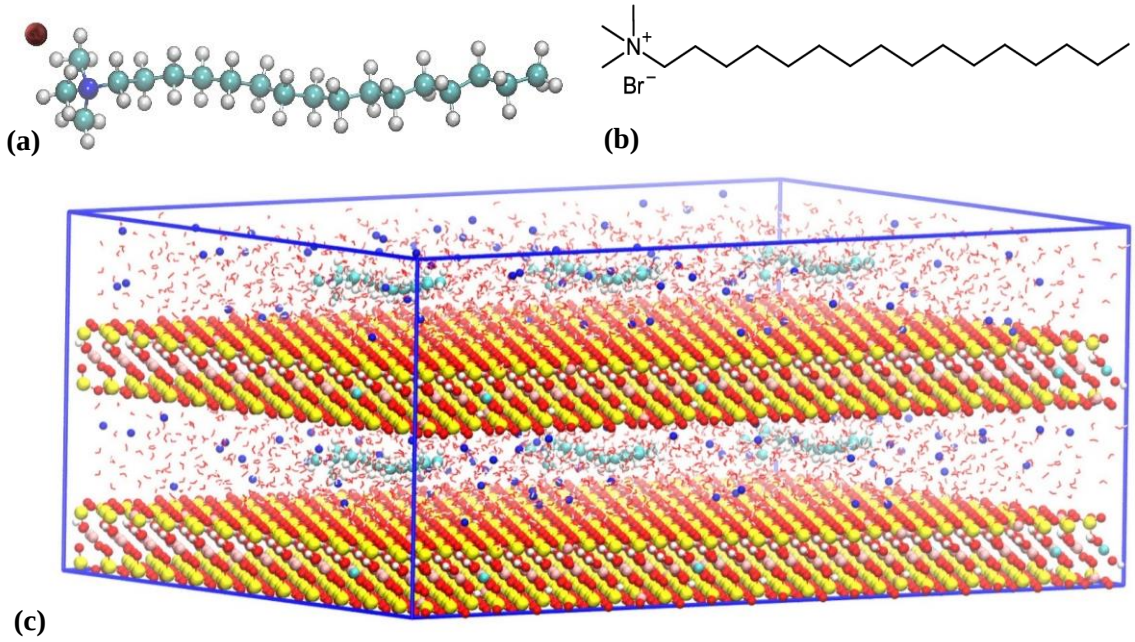

Figure 1. (a) CTAB molecule snapshot, (b) structural formula of CTAB, and (c) snapshot of simulation system (Na-MMT color: yellow for Si, pink for Al, cyan for Mg, red for O, white for H, and blue for Na^+ and CTAB color: cyan for C, white for H, reddish black for Br^-, and blue for N).

3. Results and Discussion

3.1. Swelling rate variation

To characterize the impact of CTAB on reducing MMT swelling at the last stage of crystalline state in the presence of 3W layer hydrate, the basal spacing, denoted as *d* (Å), represents the distance between the lower surfaces of two consecutive clay layers, is determined. **Table 2** presents the basal spacing results for the different systems under investigation. The basal spacing for Na-MMT (3W) without any inhibitor is 19.3 Å, which is consistent with values mentioned in existing literature (Chang et al., 1998b; Sun et al., 2015). Slight variations in the obtained *d*-spacing values in different MD studies can be attributed to differences in the considered chemical structures of Na-MMT.

Regarding the impact of CTAB inhibitor, the results show that *d*-spacing is reduced by 4.14% and 5.18% for CTAB concentrations of 6 and 10 g/L concentrations, respectively. Leveraging the double effects of KCl and CTAB demonstrates that the addition of KCl in the presence of CTAB can effectively further reduce *d*-spacing. However, it is important to note that higher concentrations of KCl do not necessarily lead to greater reduction in the interlayer space. As shown in **Table 2**, for 6 g/L CTAB, the addition of KCl with concentration of 5 and 8 wt%, can reduce *d*-spacing by 6.21% and 8.29%, respectively, which is approximately 2 to 4% more than the reduction achieved by pure 6 g/L CTAB. Such an impact of KCl is also valid for the higher concentration of CTAB, i.e., 10 g/L, with almost the same extra reduction in *d*-spacing. However, the reverse relation is observed for the impact of KCl on clay swelling when the KCl concentration increases to 12 wt%. In more detail, for both assessed concentrations of CTAB, when KCl concentration increases to 12 wt%, the dual impacts for clay swelling reduction are diminished, in which higher reduction in swelling is no longer achieved by increasing KCl over 8 wt%. To scrutinize the reason behind such behaviors of

KCl and CTAB, we first assess the molecular configuration of components via density profile analysis.

Table 2. Basal spacing *d*-value (Å) of various studied simulation systems. The reference for comparison of impacts of inhibitor is Na-MMT with 3W hydrate layer and equilibrated *d*-spacing value of 19.3 Å.

System	*d*-spacing (Å)	Changes in *d*-spacing
Water + Na-MMT +	After equilibration state	%
6 g/L CTAB	18.5	4.14
6 g/L CTAB + 5 wt% KCl	18.1	6.21
6 g/L CTAB + 8 wt% KCl	17.7	8.29
6 g/L CTAB + 12 wt% KCl	17.9	7.25
10 g/L CTAB	18.3	5.18
10 g/L CTAB + 5 wt% KCl	18.0	6.73
10 g/L CTAB + 8 wt% KCl	17.6	8.80
10 g/L CTAB + 12 wt% KCl	17.8	7.72

3.2. Distribution of interlayer components

To gain deeper insight into the reason behind the behavior of CTAB and the impact of concentration, we performed a comparative analysis of the molecular arrangement of different components in the z-direction, which is perpendicular to the clay layers. Specifically, we analyzed the distribution of the oxygen atom in water (O_w), hydrogen atom of water molecules (H_w), nitrogen of CTAB (N_{CTAB}), tail of CTAB (C_{CTAB}), and interlayer cations (Na^+). **Figure 2** shows the distribution of O_w for three cases of pure water, 6 g/L CTAB, and 10 g/L CTAB. The presence of three distinct peaks in the distribution of O_w confirms the formation of 3W hydration layers in all simulated cases. Here, the distribution of water molecules in the absence of the inhibitors is greatly in line with the literature (Kadoura et al., 2016). Interestingly, it is evident that the addition of CTAB results in a more compact arrangement of the water layers, and this is intensified by increasing the CTAB concentration. According to **Figure 2**(b), which demonstrates the distribution of H_w, the addition of CTAB leads to relocating a portion of water molecules close to the surface towards the middle of the interlayer. In the absence of CTAB, two small peaks of H_w are observed close to the clay surface along with three peaks associated with 3W hydrate layers, which indicate strong affinity of water molecules

towards the surface. When CTAB was added to the interlayer, the small peaks were observed in the distribution of H_w. This phenomenon can be ascribed to the electrostatic interactions between the CTA^+ cations and the surface of the slab, which overcome the interplays between H_w and the slab surface with the negative charge. In other words, CTAB not only acts to partially neutralize the negative charge of layers but also hinders the water molecules' adsorption onto the clay surface. This observation becomes more pronounced at the higher CTAB concentration, i.e., 10 g/L. This is also confirmed by comparing the number of hydrogen bonds (H-bonds) between water and the clay surface, as shown in **Figure S3**. Moreover, the presence of more CTA^+ in interlayers results in a disruption in the distribution of water molecules at the middle of interlayer. This interference is attributed to the presence of the CTAB tail and its structural hindrance. It should be noted that the differences in distribution of H_w near the surface in systems with CTAB is due to variation in charge distribution of the clay layer.

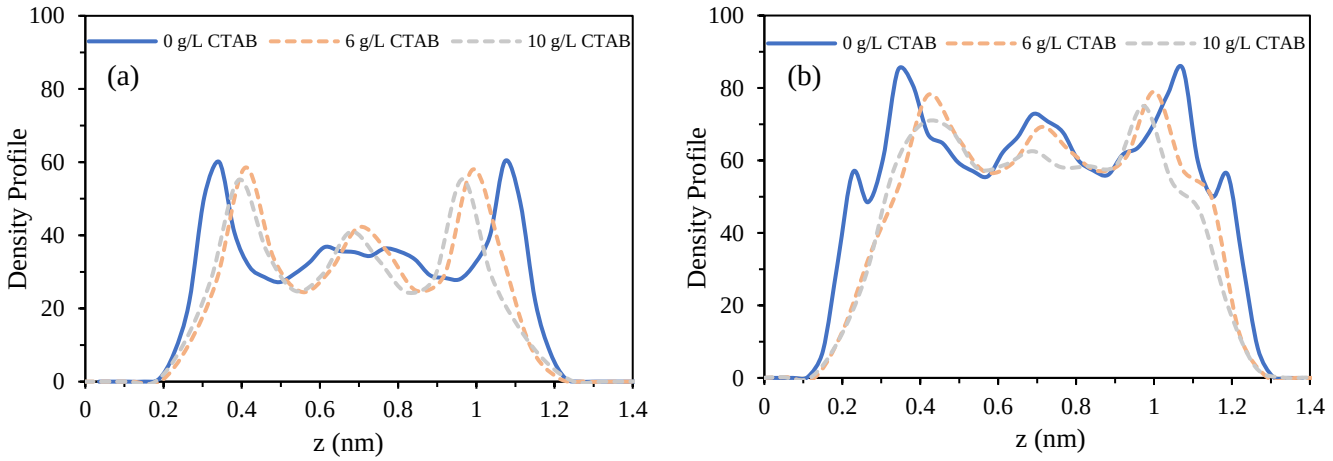

Figure 2. Density profiles of (a) O_w and (b) H_w for three cases of 0 g/L, 6 g/L, and 10 g/L CTAB.

Figure 3 demonstrates the distribution of CTAB molecules, specifically the tail of CTAB (carbon chain) represented by solid lines and the head of CTAB (nitrogen atom) represented by dashed lines, along with the interlayer cations (Na^+). Although it was expected that the CTA^+ molecule would interact with the clay surface through its positively charged head, **Figure 3**(a) shows that both the

tail and head of the CTA^+ molecule are at the same distance from the clay surface, indicating the parallel orientation of CTA^+ monolayer with the surface (see **Figure 3**(c)). This parallel alignment of the CTA^+ cation justified the relocation of some of the water molecules towards the interlayer. Notably, a greater accumulation of CTA^+ cations close to the surface is observed at the higher concentration (10 g/L). Therefore, it can be concluded that the configurational arrangement of CTA+ not only leads to the repositioning of water molecules from the surface but also compels the Na+ cations at the interface to move towards the middle of the layers. **Figure 3**(b) illustrates that without CTAB, there are five different layers of Na^+ cations where two layers are distributed close to Na-MMT, forming inner-sphere surface complex (ISSC). Given that outer-sphere surface complexes (OSSCs) are established where the distance of ions is more than 3 Å from the clay slab (Lammers et al., 2017), it can be observed that two OSSCs confined between water layer in conjugated with a layer at the middle interlayer are formed. Interestingly, in the presence of CTAB, the five layers of interlayer cations are converted to the four layers, in which the middle layer of the latter case disappears while there are still two ISSCs and OSSCs for both concentrations of CTAB. Furthermore, the structural position of the CTA^+ monolayer leads to a higher accumulation of Na^+ cations within the interlayer's center.

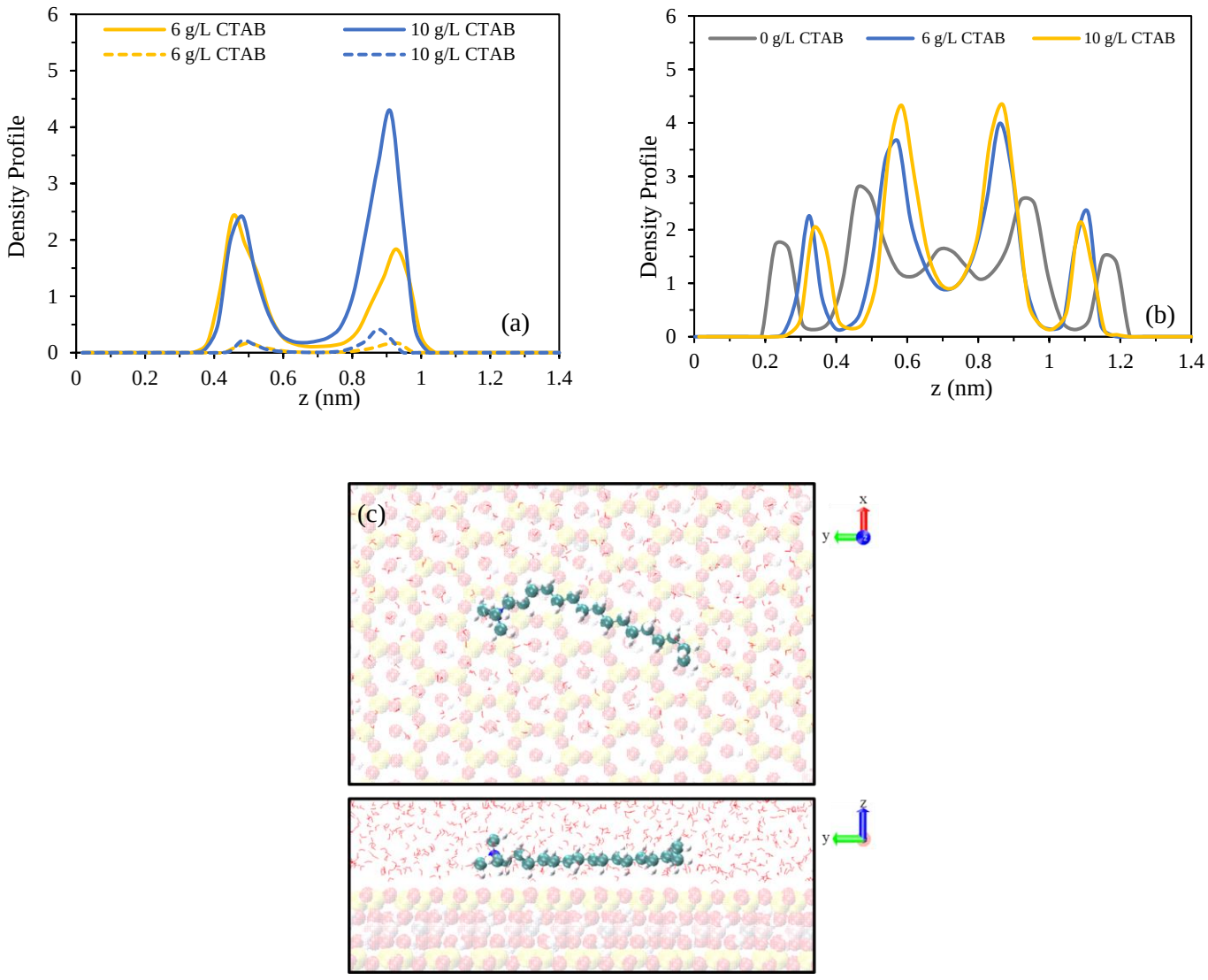

Figure 3. Density Profile of (a) tail of CTAB (solid line) and nitrogen of CTAB (dashed line) and (b) Na^+ cations. The monolayer configuration of CTA^+ over the clay surface is shown in part (c).

To optimize drilling fluids, it is common practice to use multiple inhibitors simultaneously, as each clay swelling inhibitor operates through specific inhibition mechanisms. Among these inhibitors, inorganic salts, particularly potassium chloride (KCl), are widely employed. KCl acts as an inhibitor by reducing clay swelling through a cation exchange mechanism (Swai, 2020). Interestingly, it has been observed that the addition of KCl does not necessarily enhance the inhibitory properties when CTAB is already present. **Figure 4** demonstrates the distribution of water (H_w and O_w) and interlayer cations (Na^+ and K^+) for a concentration of 10 g/L CTAB. The density profiles of H_w and O_w remain

identical regardless of the concentration of KCl added. However, the positions of Na^+ and K^+ cations differ and are influenced by the concentration of KCl. Generally, K^+ cations demonstrate a more pronounced inclination to stay in proximity to the clay surface when compared to Na^+ cations. In all cases, K^+ cations distinctly create two ISSCs with varying degrees of accumulation near the surface. In the coactions of CTAB (10 g/L) and KCl (5 wt%), owing to interactions between K^+ ions and the clay surface, some of the Na^+ cations are repelled from the surface, and as it is evident from **Figure 4**(b), more Na^+ cations are present in the form of OSSCs compared to **Figure 4**(a), the case with no KCl. It is worth noting that the distribution of K^+ cations are not just restricted near the surface, and some K^+ cations are uniformly placed around the middle of the interlayer. Addition of more KCl, i.e., 8% wt., has no significant impact on the distribution of Na^+ cations near the surface, and the majority of K^+ cations are distributed around the middle of the interlayer as it is shown by higher intensity of OSSCs in **Figure 4**(b). However, when the concentration of KCl increases to 12%., a notable change occurs in the arrangement of Na^+ cations. The majority of Na^+ cation, which was previously positioned in proximity to the clay surface in lower KCl concentrations, are transferred to the center to form more OSSCs. The divergent swelling behavior of these systems can be attributed to the intrinsic distinction in the hydration enthalpies between Na^+ and K^+ cations. Given that hydration enthalpy of Na^+ cations (-406 $kJ.mol^{-1}$) is more than that of K^+ cations (-320 $kJ.mol^{-1}$), they can form fairly stable hydration shell, which results in fully hydrated ions. This means that the presence of more K^+ cation compared to Na^+ cations should provide more inhibition. This happened up to 8 wt% in the presence of CTAB where no considerable changes occur for Na^+ cation forming ISSCs. However, the presence of excessive amount of K^+ cations, which replaced the majority of Na^+ cations by breaking their interactions with the clay surface, does not necessarily improve the inhibition property.

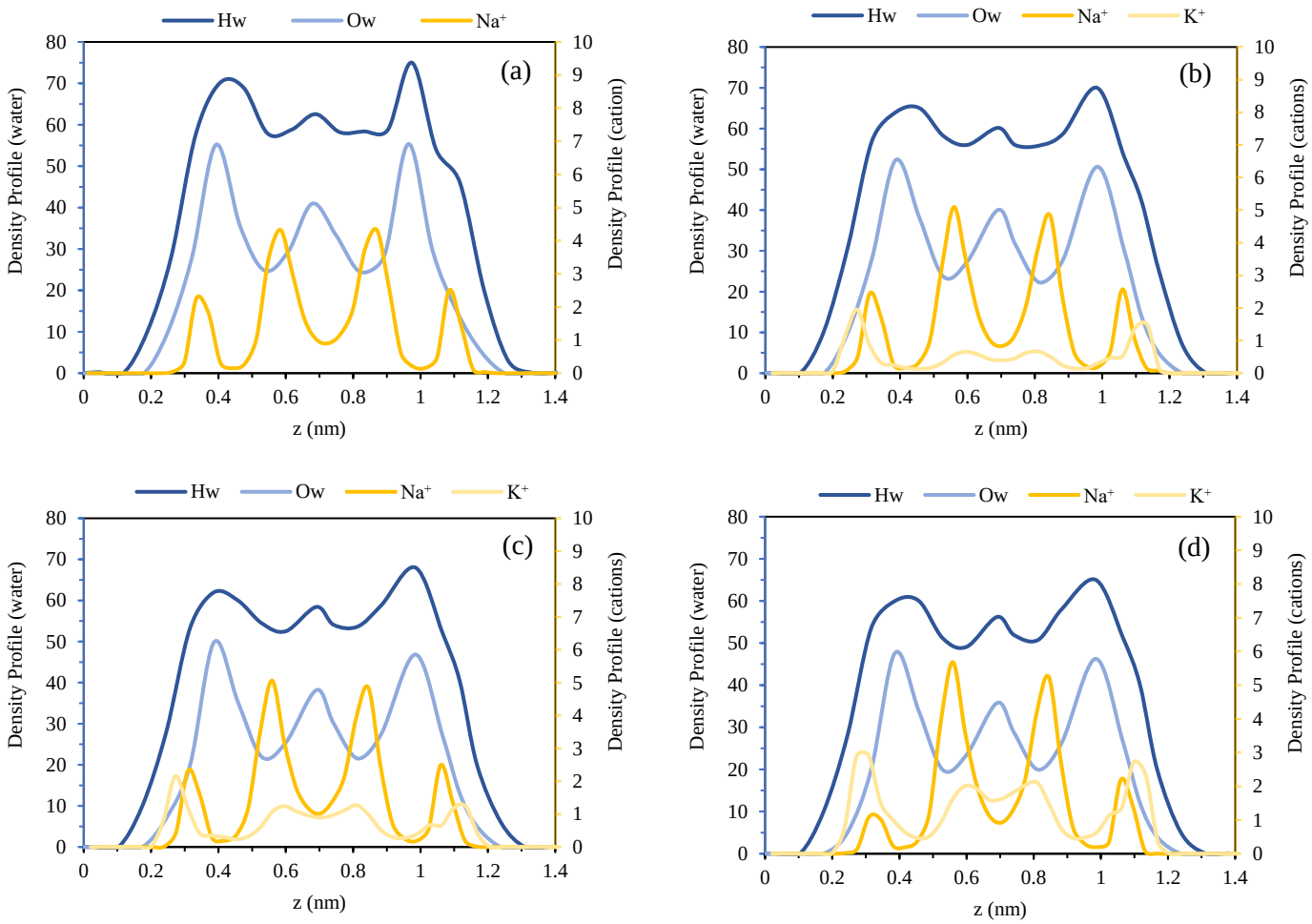

Figure 4. Density profile of water (H_w and O_w) and interlayer cations (Na^+ and K^+) for (a) 12 g/L CTAB + 0 wt% KCl, (b) 12 g/L CTAB + 5 wt% KCl, (c) 12 g/L CTAB + 8 wt% KCl, and (d) 12 g/L CTAB + 12 wt% KCl. As it is evident, addition of KCl up to 12 wt% caused relocating more Na^+ cations into the interlayer's center, which means higher possibility of hydration of cations and then clay swelling.

3.3. Molecular pair distance

To obtain further insight into the interactions between specific pairs of the atoms and their distributions, radial distribution functions (RDFs) were evaluated. **Figure 5** presents RDFs of Na^+-O_b and H_w-O_b in Na-MMT systems with varying concentrations CTAB. Comparing the interactions of Na^+-O_b and H_w-O_b with the main RDF peak location of 0.27 nm and 0.20 nm, respectivley, shows that water molecules exhibit a greater inclination to be in proximity to the slab compared to Na^+ cations, even after adding CTAB. This is due to high polarizibility of the MMT surface stemmed

from the isomohrphic substituions in the O-sheet. Neverthless, the presence of CTAB in the interlayers can influence the intensity of interactions in pairs of atoms. As depicted in **Figure 5**(a), the RDF of Na^+ cations with the O_b exhibits a gradual decrease with the addition of CTAB, indicating relocating Na^+ cations towards the middle of the interlayers. This observation aligns with the Na^+ density profile shown in **Figure 3**(b). Similarly, the presence of CTAB removes some water from the clay surface and pushes them towards the middle. As previously discussed, CTAB molecules align in a parallel manner with the clay surface, contributing to this effect. The point that should be referred is that although CTAB can relocate the interlayer cations and water molecules, among CTA^+ cations, Na^+ cations, and H_w, the initial major peak of CTA^+ cations is positioned at further distance (**Figure 3**(c)). Nevertheless, the interactions of CTA^+ molecules with the clay surface occur without any mediation by water or Na^+ cations. Regarding the relocation of water and Na^+ cations by CTAB, two indirect interpretations can be drawn. First, relocating Na^+ cations from the clay surface promotes the capability of CTA^+ cations to follow the cation exchange mechanism. Second, the presence of the lower amount of water close to the surface improves CTAB's potential in altering wettability of the surface. We mentioned indirect interpretations because the simulation systems in this study were not designed to allow water molecules to move outside or penetrate inside the interlayers and reach a direct conclusion. Regarding the inhibition mechanism of CTAB, however, one may expect that transferring both Na^+ cations and water molecules to the middle of interlayer should have imposed further swelling as a result of higher hydration, as shown in **Figure S4**, where the higher RDF has been obtained for Na^+-O_w pairs at the higher CTAB concentration. Nevertheless, the origin of inhibition mechanism of CTAB can be scrutinized in the orientation of CTA^+ molecules. The snapshot of equilibrium state of the system containing 10 g/L CTAB (**Figure 3**(d)) shows that parallel orientations of CTA^+ molecules (bilayer) with respect to the surface keep the

clay layers together. This means that the positive impact of molecular orientation of CTA^+ on swelling performance is more than the adverse effect of relatively higher cation hydration.

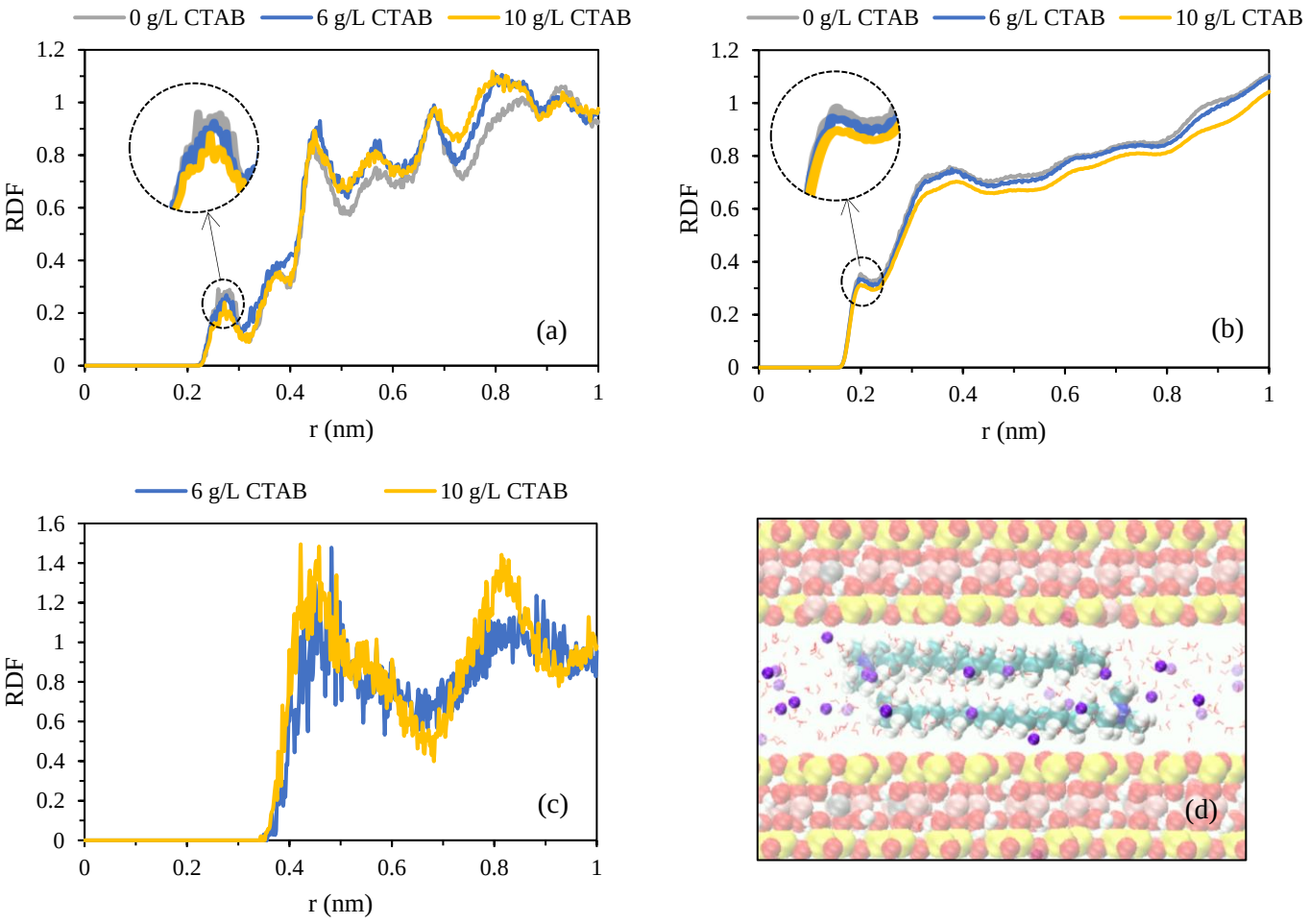

Figure 5. Profiles of RDF for (a) Na^+-O_b, (b) H_w-O_b, and (c) N_{CTAB}-O_b for different system containing various CTAB concentrations. As it is evident, addition of CTAB resulted in removing of Na^+ cations and water from the clay surface. Special parallel orinentation of CTA^+ molecules with repsective to the clay surface is shown in part (d).

Figure 6(a) and **6**(b) show the RDFs of the counterions, i.e., Na^+ and K^+ with O_s and O_w, respectively, for various KCl concentrations. As shown in **Figure 6**(a), for all cases, although Na^+ cations are in closer proximity to the clay surface in contrast to K^+ cations, their presence is characterized by a lower intensity than that of K^+ cations. The variance in the positioning of the initial peak arises from variations in the ionic radii of the cations, which is higher for K^+ cations (Rahromostaqim and Sahimi, 2018). In the presence of KCl concentrations, the interactions between

Na^+ cations and the clay surface are diminished due to the influence of elevated K^+ cations, and on the contrary, more accumulation of K^+ cations is observed at the clay surface. Such behaviors of counterions are mainly due to the difference in the enthalpy of hydration that we previously explained. Indeed, most K^+ cations stay near the MMT surface and have no tendency to be hydrated by water molecules. Conversely, Na^+ cations can easily be hydrated by water, and they can form larger hydration shells, which causes clay swelling. As shown in **Figure 6**(b), the initial hydration shells of cations-O_w appear at 2.38 ± 0.02 Å and 2.78 ± 0.02 Å for Na^+ and K^+, respectively, which align with findings from prior research investigations (Boulet et al., 2004; Denis et al., 1991). Note that at the higher KCl concentration, i.e., 12 wt%, the greater RDF peak occurs for Na^+ cations and water molecules, which corroborates the density profile outcomes. This worsens the combined inhibitory effect of CTAB and KCl compared to lower KCl concentrations.

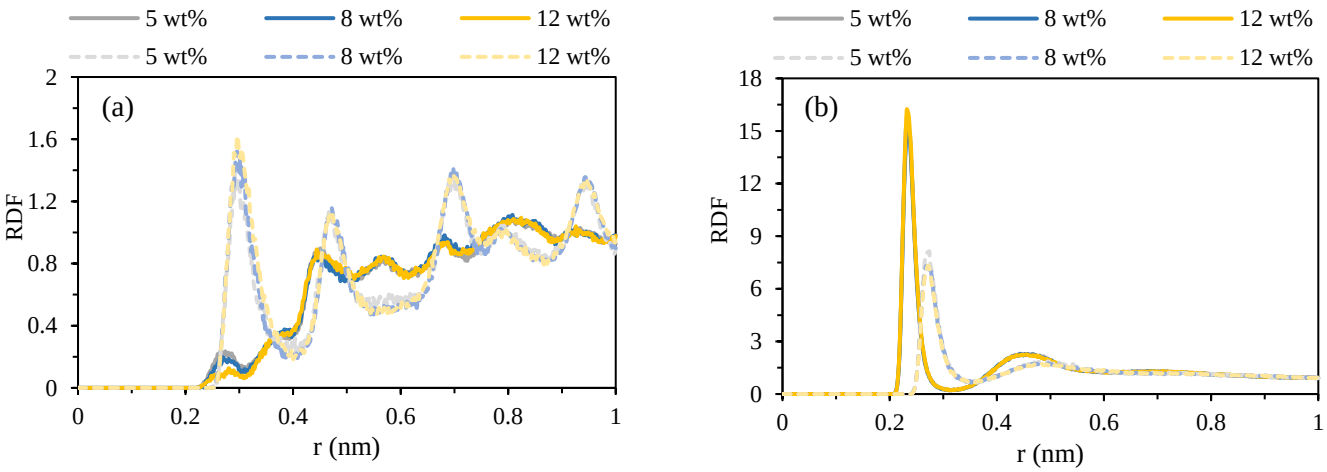

Figure 6. RDF curves for (a) Na^+-O_b (solid line) and K^+-O_b (dashed line), and (b) Na-O_w (solid line) and K-O_w (dashed line) for 10 g/L CTAB and various concentrations of KCl.

3.4. Charge density of clay surface

The negative charge of clay layers can form an electrical double layer (EDL) over the surface (Laird, 2006). The higher the EDL length near the clay surface means the greater the affinity of the MMT surface to adsorb water dipoles due to the electric potential difference. Hence, it enhances the

accumulation of water molecules near the surface, or in another interpretation, the penetration of more water into the clay interlayers (Smalley, 1994). This increase in water accumulation near the clay surfaces leads to enhanced clay swelling. Consequently, reducing the electric charge on the clay surface can effectively control clay swelling. As shown in **Figure 7**, when CTAB is added to the system, the negative charge on the surface reduces by creating a monolayer and bilayer structures over the clay surface. Specifically, without CTAB molecules, the charge over the surface is -220.15 $q.nm^{-3}$, and it gradually decreases to -150.14 $q.nm^{-3}$ and -110.05 $q.nm^{-3}$ by adding 6 g/L and 10 g/L CTAB. Indeed, this shows that the inhibitory performance of CTAB cannot be attributed to a single mechanism alone. Instead, CTAB employs multiple inhibition mechanisms simultaneously to effectively reduce clay swelling. It can be inferred that even though addition of CTAB may change the location of Na^+ cations to be exposed more to the hydration, positive contributions of other mechanisms outweigh the adverse effects of cation hydration on clay swelling. Additionally, the presence of KCl can also further reduce the surface charge density. However, the effectiveness of KCl in altering surface charge density is not as significant as that of CTAB. Reduction of the surface charge at the higher KCl concentration is not substantial, in which the surface charge density reaches to -86.15 $q.nm^{-3}$ at 12 %wt KCl from -101.32 $q.nm^{-3}$ at 5 %wt KCl. This limited reduction may explain the reverse performance of KCl at 12%wt in the presence of CTAB, as it is unable to compensate for the negative impact of the relocation of Na^+ cations towards the middle of the interlayer.

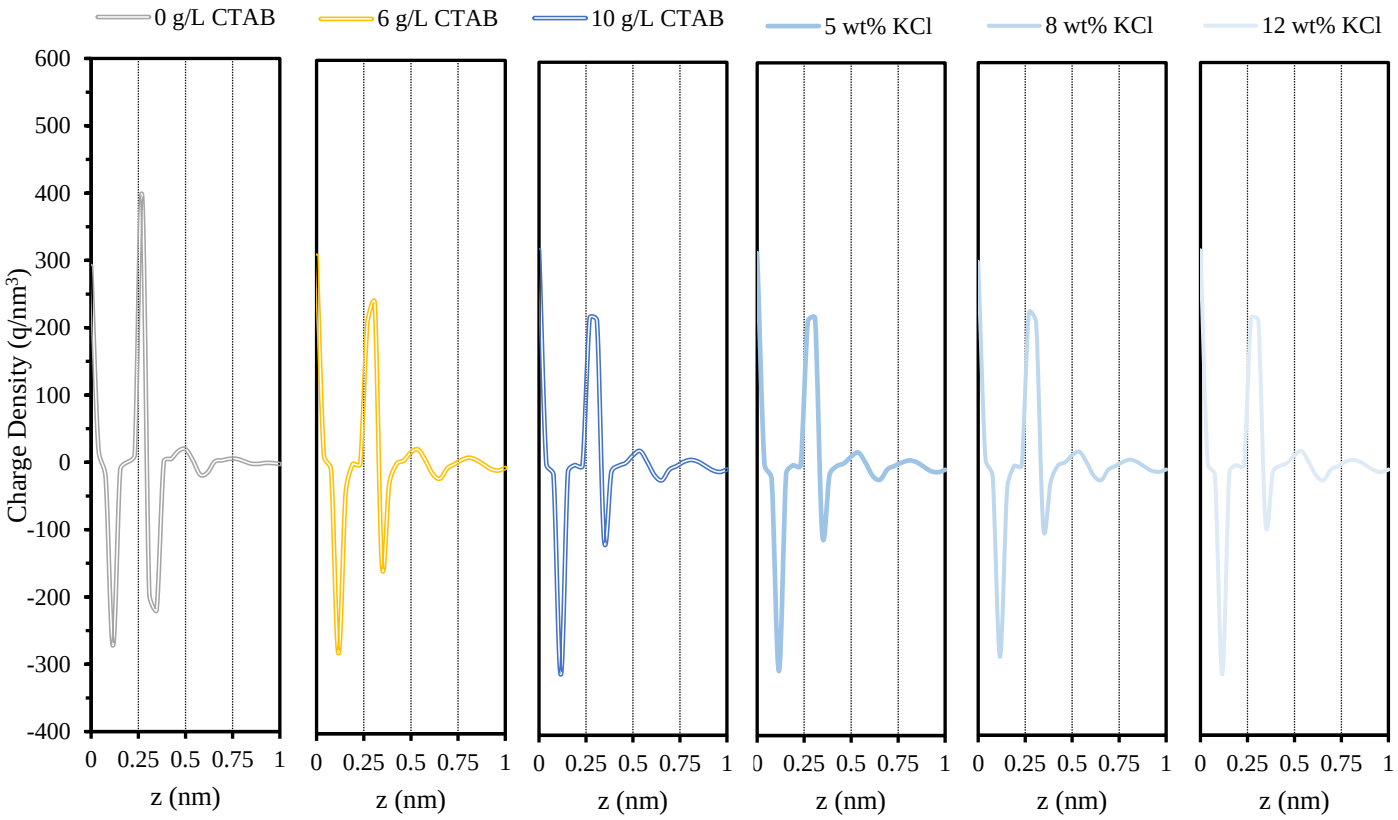

Figure 7. Charge density distribution of the system along z-axis (perpendicular to the clay surface) for various concentrations of CTAB. The impact of KCl concentration was considered in the presence of 10 g/L CTAB. Note that z starts from the middle of one clay slab (O-sheet) towards the middle of the interlayers.

3.5. Movement of interlayer water

The diffusivity of water molecules in clay interlayers exerts a substantial influence on the swelling characteristics of MMT. Minimizing water mobility is crucial, as higher mobility leads to increased swelling by exerting greater swelling pressure (Sun et al., 2016). To assess the effects of the added inhibitor on the dynamic characteristics of water molecules, the mean-squared displacement (*MSD*) analysis was used to obtain self-diffusion coefficients (D_s) (Marry and Turq, 2003). The *MSD* profile of water for different studied cases is illustrated in **Figure 8**(a). As evident, the slope of the *MSD* curves gradually decreases with addition of CTAB in different concentrations , indicating that CTAB can restrict the water molecules' movement. Similarly, KCl exhibits a similar effect, as lower *MSD* slopes are observed with higher KCl concentrations. Comparing the diffusion of water molecules in

Figure 8(b) demonstrates that an addition of CTAB reduces the D_s of water from 1.9×10^{-9} $m^2.s^{-1}$ to 1.65×10^{-9} and 1.52×10^{-9} $m^2.s^{-1}$ for lower and higher concentrations of CTAB, respectively. The impact of KCl on diffusivity of water molecules in the presence of 10 g/L CTAB shows a reduction trend by 13 %, 25%, and 34% for lower to higher studied KCl concentrations. These findings confirm the previous results. Indeed, the presence of CTAB acts as a hindrance for water molecules by creating the monolayer and bilayer structures parallel to the slab. Addition of KCl can also further impose restriction to the movement of water molecules due to their interactions with counterions with lower enthalpy of hydrations.

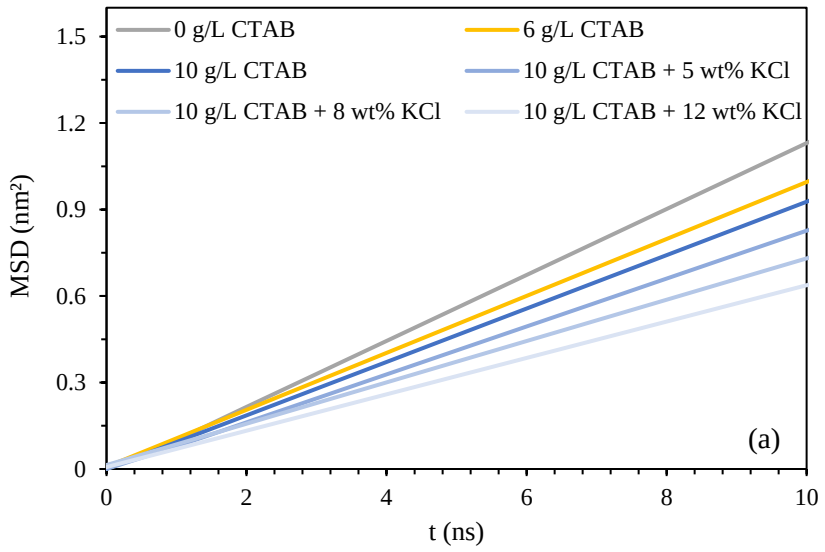

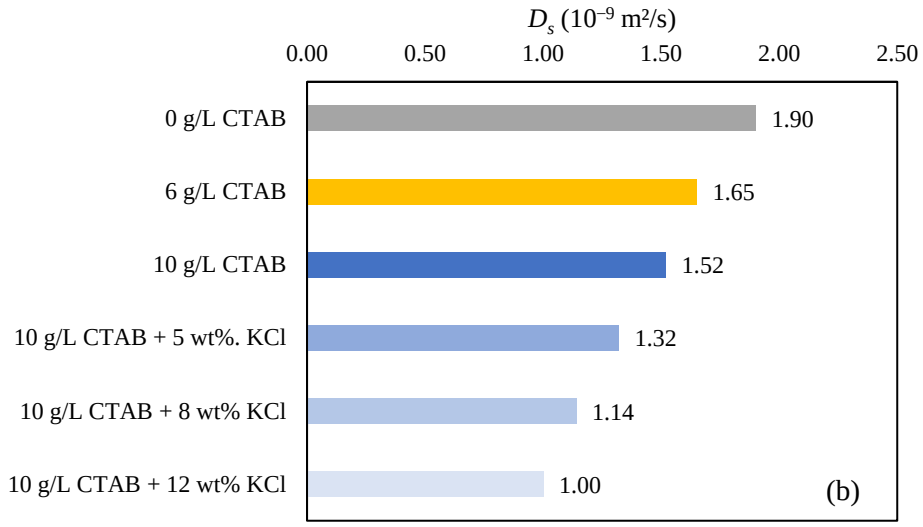

Figure 8. Comparison of (a) *MSD* and (b) D_s of water molecules in different studied cases. As it is evident, the presence of more CTAB and KCl acted as a barrier for water movement.

4. Implications for subsurface drilling

Subsurface drilling with perspectives of petroleum extraction, geothermal energy, gas storage, etc., is amongst the expensive processes of reaching the reservoirs. Neglecting the accurate optimization of these sections can result in significant challenges, leading to higher expenses or even failure to reach the desired target. Among these challenges, dealing with expandable clay swelling in subsurface formations is of utmost importance. Ensuring the success of the drilling operation hinges on the critical optimization of the drilling fluid, which is essential for effectively controlling clay swelling. This study highlights the significance of optimizing the simultaneous impacts of clay swelling inhibitors, namely CTAB and KCl, in postponing the shift from a crystalline swelling state to an osmotic swelling state. The addition of CTAB can reduce clay swelling by formation of monolayer and bilayer structures parallel to the slab surface. This restructuring is coupled with the relocation of Na^+ cations and water molecules, which are moved further away from the clay surface.

This phenomenon enhances the CTAB potential in cation exchange and alteration of surface wetness, respectively. Despite the higher susceptibility of Na^+ cations to hydration within the middle of the interlayers, specific orientations of CTAB effectively maintain the close proximity of the clay layers. Furthermore, CTAB compensates for the negative charge present on the clay surface and acts as an impediment for movement of the water molecules. This indicates that the effects of CTAB in the interlayer are not solely positive, but the overall positive impacts outweigh the negatives, leading to a reduction in clay swelling. The addition of KCl, an early solution to counteract clay swelling, in combination with CTAB can enhance the inhibition performance. Indeed, K^+ cations, which predominantly undergo cation exchange, replace the Na^+ cations near the clay surface. Having lower enthalpy of hydration compared to Na^+ cations, K^+ cations up to the middle concentration (8 wt%) can positively contribute to swelling reduction in the presence of CTAB. However, the detrimental impact of further removing of Na^+ cations from the surface due to the presence of more and more K^+ cations in the interlayers can deteriorate the combined impacts of CTAB and KCl due to formation of larger hydration shells of Na^+ cations. This implies that using higher concentration of KCl is not always the solution even for the most expandable type of clay minerals.

5. Conclusions

In this study, molecular dynamics (MD) simulation was utilized to investigate how the presence of CTAB surfactant inhibits the swelling of Na-MMT. Furthermore, the study examined the combined impacts of KCl and CTAB at standard concentrations of 5 wt%, 8 wt%, and 12 wt%. The findings indicated that the addition of 6 and 10 g/L CTAB led to a reduction in the d-spacing value from 19.3 Å (without the inhibitor) to 18.5 and 18.3 Å, respectively. The arrangement of monolayer and bilayer CTA^+ molecules in parallel to the slab surface results in the displacement of Na^+ ions and water from the clay surface. This suggests a cation exchange mechanism and alters the wetness properties, making it less hydrophilic. Additionally, further compensation of the clay surface charge positively contributes to reducing clay swelling. The performance of CTA^+ cations is improved by adding KCl at 5 and 8 wt%. Yet, the enhanced effectiveness of the combined inhibitors diminishes at 12 wt% KCl. At this concentration, the elevated ratio of K^+ to Na^+ leads to a shift in the form of Na^+ cations from ISSCs near the surface to OSSCs farther from the surface. This increases the likelihood of higher hydration for Na^+ cations, thereby negatively impacting the combined performance of CTAB and KCl.

CRediT authorship contribution statement

Mehdi Karimi: Software, formal analysis, visualization, validation, data curation, and writing – original draft. **Mehdi Ghasemi**: Conceptualization, methodology, investigation, writing-review & editing, and supervision. **Masoud Babaei**: Writing-review & editing. **Khalil Shahbazi**: Conceptualization, writing-review & editing, and supervision. All authors have read and agreed to the published version of the manuscript**.**

References

Abbas, M.A., Zamir, A., Elraies, K.A., Mahmood, S.M. and Rasool, M.H., 2021. A critical parametric review of polymers as shale inhibitors in water-based drilling fluids. Journal of Petroleum Science and Engineering, 204: 108745.

Ahmad, H.M., Murtaza, M., Shakil Hussain, S.M., Mahmoud, M. and Kamal, M.S., 2023. Performance evaluation of different cationic surfactants as anti-swelling agents for shale formations. Geoenergy Science and Engineering, 230: 212185.

Ahmed, H.M., Kamal, M.S. and Al-Harthi, M., 2019. Polymeric and low molecular weight shale inhibitors: A review. Fuel, 251: 187-217.

Ahmed Khan, R., Murtaza, M., Abdulraheem, A., Kamal, M.S. and Mahmoud, M., 2020. Imidazolium-Based Ionic Liquids as Clay Swelling Inhibitors: Mechanism, Performance Evaluation, and Effect of Different Anions. ACS Omega, 5(41): 26682-26696.

Barati, P., Shahbazi, K., Kamari, M. and Aghajafari, A., 2017. Shale hydration inhibition characteristics and mechanism of a new amine-based additive in water-based drilling fluids. Petroleum, 3(4): 476-482.

Bi, Z., Zhang, Z., Xu, F., Qian, Y. and Yu, J., 1999. Wettability, Oil Recovery, and Interfacial Tension with an SDBS–Dodecane–Kaolin System. Journal of Colloid and Interface Science, 214(2): 368-372.

Bjelkmar, P., Larsson, P., Cuendet, M.A., Hess, B. and Lindahl, E., 2010. Implementation of the CHARMM Force Field in GROMACS: Analysis of Protein Stability Effects from Correction Maps, Virtual Interaction Sites, and Water Models. Journal of Chemical Theory and Computation, 6(2): 459-466.

Boulet, P., Coveney, P.V. and Stackhouse, S., 2004. Simulation of hydrated Li+-, Na+- and K+-montmorillonite/polymer nanocomposites using large-scale molecular dynamics. Chemical Physics Letters, 389(4): 261-267.

Bourg, I.C. and Sposito, G., 2011. Molecular dynamics simulations of the electrical double layer on smectite surfaces contacting concentrated mixed electrolyte (NaCl–CaCl2) solutions. Journal of Colloid and Interface Science, 360(2): 701-715.

Bussi, G., Donadio, D. and Parrinello, M., 2007. Canonical sampling through velocity rescaling. The Journal of chemical physics, 126(1): 014101.

Camara, M. et al., 2017. Molecular dynamics simulation of hydrated Na-montmorillonite with inorganic salts addition at high temperature and high pressure. Applied Clay Science, 146: 206-215.

Chang, F.-R.C., Skipper, N. and Sposito, G., 1995. Computer simulation of interlayer molecular structure in sodium montmorillonite hydrates. Langmuir, 11(7): 2734-2741.

Chang, F.-R.C., Skipper, N. and Sposito, G., 1998a. Monte Carlo and molecular dynamics simulations of electrical double-layer structure in potassium− montmorillonite hydrates. Langmuir, 14(5): 1201-1207.

Chang, F.-R.C., Skipper, N.T. and Sposito, G., 1998b. Monte Carlo and Molecular Dynamics Simulations of Electrical Double-Layer Structure in Potassium−Montmorillonite Hydrates. Langmuir, 14(5): 1201-1207.

Chenevert, M.E., 1970. Shale alteration by water adsorption. Journal of petroleum technology, 22(09): 1141-1148.

Cygan, R.T., Greathouse, J.A. and Kalinichev, A.G., 2021. Advances in Clayff Molecular Simulation of Layered and Nanoporous Materials and Their Aqueous Interfaces. The Journal of Physical Chemistry C, 125(32): 17573-17589.

Cygan, R.T., Liang, J.-J. and Kalinichev, A.G., 2004. Molecular Models of Hydroxide, Oxyhydroxide, and Clay Phases and the Development of a General Force Field. The Journal of Physical Chemistry B, 108(4): 1255-1266.

Dazas, B. et al., 2015. Influence of Tetrahedral Layer Charge on the Organization of Interlayer Water and Ions in Synthetic Na-Saturated Smectites. The Journal of Physical Chemistry C, 119(8): 4158-4172.

de Lara, L.S., Rigo, V.A. and Miranda, C.R., 2017. Controlling Clay Swelling–Shrinkage with Inorganic Nanoparticles: A Molecular Dynamics Study. The Journal of Physical Chemistry C, 121(37): 20266-20271.

Denis, J., Keall, M., Hall, P. and Meeten, G., 1991. Influence of potassium concentration on the swelling and compaction of mixed (Na, K) ion-exchanged montmorillonite. Clay Minerals, 26(2): 255-268.
Du, J., Zhou, A., Lin, X., Bu, Y. and Kodikara, J., 2020. Revealing Expansion Mechanism of Cement-Stabilized Expansive Soil with Different Interlayer Cations through Molecular Dynamics Simulations. The Journal of Physical Chemistry C, 124(27): 14672-14684.
Frenkel, D., Smit, B. and Ratner, M.A., 1996. Understanding molecular simulation: from algorithms to applications, 2. Academic press San Diego.
Ghamartale, A., Rezaei, N. and Zendehboudi, S., 2023. Alternation of asphaltene binding arrangement in the presence of chemical inhibitors: Molecular dynamics simulation strategy. Fuel, 336: 127001.
Ghamartale, A., Zendehboudi, S. and Rezaei, N., 2020. New Molecular Insights into Aggregation of Pure and Mixed Asphaltenes in the Presence of n-Octylphenol Inhibitor. Energy & Fuels, 34(10): 13186-13207.
Ghasemi, M. et al., 2019. Primary evaluation of a natural surfactant for inhibiting clay swelling. Journal of Petroleum Science and Engineering, 178: 878-891.
Ghasemi, M. and Shafiei, A., 2022. Influence of brine compositions on wetting preference of montmorillonite in rock/brine/oil system: An in silico study. Applied Surface Science, 606: 154882.
Ghasemi, M., Shafiei, A. and Foroozesh, J., 2022. A systematic and critical review of application of molecular dynamics simulation in low salinity water injection. Advances in Colloid and Interface Science, 300: 102594.
Ghasemi, M. and Sharifi, M., 2021. Effects of layer-charge distribution on swelling behavior of mixed-layer illite-montmorillonite clays: A molecular dynamics simulation study. Journal of Molecular Liquids, 335: 116188.
Gholami, R., Elochukwu, H., Fakhari, N. and Sarmadivaleh, M., 2018. A review on borehole instability in active shale formations: Interactions, mechanisms and inhibitors. Earth-Science Reviews, 177: 2-13.
Greathouse, J.A., Cygan, R.T., Fredrich, J.T. and Jerauld, G.R., 2016. Molecular dynamics simulation of diffusion and electrical conductivity in montmorillonite interlayers. The Journal of Physical Chemistry C, 120(3): 1640-1649.
Hensen, E., Tambach, T., Bliek, A. and Smit, B., 2001. Adsorption isotherms of water in Li–, Na–, and K–montmorillonite by molecular simulation. The Journal of Chemical Physics, 115(7): 3322-3329.
Humphrey, W., Dalke, A. and Schulten, K., 1996. VMD: Visual molecular dynamics. Journal of Molecular Graphics, 14(1): 33-38.
Jia, H. et al., 2019. Investigation of inhibition mechanism of three deep eutectic solvents as potential shale inhibitors in water-based drilling fluids. Fuel, 244: 403-411.
Jiafang, X. et al., 2014. Molecular simulation for inorganic salts inhibition mechanism on montmorillonite hydration. Acta Petrolei Sinica, 35(2): 377.
Kadoura, A., Narayanan Nair, A.K. and Sun, S., 2016. Molecular Dynamics Simulations of Carbon Dioxide, Methane, and Their Mixture in Montmorillonite Clay Hydrates. The Journal of Physical Chemistry C, 120(23): 12517-12529.
Laird, D.A., 2006. Influence of layer charge on swelling of smectites. Applied Clay Science, 34(1): 74-87.
Lammers, L.N. et al., 2017. Molecular dynamics simulations of cesium adsorption on illite nanoparticles. Journal of Colloid and Interface Science, 490: 608-620.
Lee, J.H. and Guggenheim, S., 1981. Single crystal X-ray refinement of pyrophyllite-1 Tc. American Mineralogist, 66(3-4): 350-357.
Li, X. et al., 2019. Application of Gelatin Quaternary Ammonium Salt as an Environmentally Friendly Shale Inhibitor for Water-Based Drilling Fluids. Energy & Fuels, 33(9): 9342-9350.
Mahto, V. and Sharma, V., 2004. Rheological study of a water based oil well drilling fluid. Journal of Petroleum Science and Engineering, 45(1-2): 123-128.
Marry, V. and Turq, P., 2003. Microscopic simulations of interlayer structure and dynamics in bihydrated heteroionic montmorillonites. The Journal of Physical Chemistry B, 107(8): 1832-1839.

Moslemizadeh, A., Aghdam, S.K.-y., Shahbazi, K., Aghdam, H.K.-y. and Alboghobeish, F., 2016. Assessment of swelling inhibitive effect of CTAB adsorption on montmorillonite in aqueous phase. Applied Clay Science, 127: 111-122.

Muhammed, N.S., Olayiwola, T. and Elkatatny, S., 2021. A review on clay chemistry, characterization and shale inhibitors for water-based drilling fluids. Journal of Petroleum Science and Engineering, 206: 109043.

Murtaza, M., Kamal, M.S. and Mahmoud, M., 2020. Application of a novel and sustainable silicate solution as an alternative to sodium silicate for clay swelling inhibition. ACS omega, 5(28): 17405-17415.

Narayanan Nair, A.K., Cui, R. and Sun, S., 2021. Overview of the Adsorption and Transport Properties of Water, Ions, Carbon Dioxide, and Methane in Swelling Clays. ACS Earth and Space Chemistry, 5(10): 2599-2611.

Norrish, K., 1954. The swelling of montmorillonite. Discussions of the Faraday society, 18: 120-134.

Nosé, S. and Klein, M., 1983. Constant pressure molecular dynamics for molecular systems. Molecular Physics, 50(5): 1055-1076.

Omrani, S. et al., 2023. Interfacial Tension–Temperature–Pressure–Salinity Relationship for the Hydrogen–Brine System under Reservoir Conditions: Integration of Molecular Dynamics and Machine Learning. Langmuir, 39(36): 12680-12691.

Quintero, L., 2002. An overview of surfactant applications in drilling fluids for the petroleum industry. Journal of dispersion science and technology, 23(1-3): 393-404.

Rahromostaqim, M. and Sahimi, M., 2018. Molecular Dynamics Simulation of Hydration and Swelling of Mixed-Layer Clays. The Journal of Physical Chemistry C, 122(26): 14631-14639.

Saleh, T.A. and Ibrahim, M.A., 2019. Advances in functionalized Nanoparticles based drilling inhibitors for oil production. Energy Reports, 5: 1293-1304.

Shi, X., Wang, L., Guo, J., Su, Q. and Zhuo, X., 2019. Effects of inhibitor KCl on shale expansibility and mechanical properties. Petroleum, 5(4): 407-412.

Skipper, N.T., Chang, F.-R.C. and Sposito, G., 1995. Monte Carlo simulation of interlayer molecular structure in swelling clay minerals. 1. Methodology. Clays and Clay minerals, 43: 285-293.

Smalley, M.V., 1994. Electrical Theory of Clay Swelling. Langmuir, 10(9): 2884-2891.

Sun, L. et al., 2016. Influence of layer charge and charge location on the swelling pressure of dioctahedral smectites. Chemical Physics, 473: 40-45.

Sun, L. et al., 2015. Molecular dynamics study of montmorillonite crystalline swelling: Roles of interlayer cation species and water content. Chemical Physics, 455: 23-31.

Suter, J., Coveney, P., Anderson, R., Greenwell, H. and Cliffe, S., 2011. Rule based design of clay-swelling inhibitors. Energy & Environmental Science, 4(11): 4572-4586.

Swai, R.E., 2020. A review of molecular dynamics simulations in the designing of effective shale inhibitors: application for drilling with water-based drilling fluids. Journal of Petroleum Exploration and Production Technology, 10(8): 3515-3532.

Tazikeh, S., Kondori, J., Zendehboudi, S., Sayyad Amin, J. and Khan, F., 2021. Molecular dynamics simulation to investigate the effect of polythiophene-coated Fe3O4 nanoparticles on asphaltene precipitation. Chemical Engineering Science, 237: 116417.

Van Der Spoel, D. et al., 2005. GROMACS: fast, flexible, and free. Journal of computational chemistry, 26(16): 1701-1718.

Vanommeslaeghe, K. et al., 2010. CHARMM general force field: A force field for drug-like molecules compatible with the CHARMM all-atom additive biological force fields. Journal of computational chemistry, 31(4): 671-690.

Wright, L.B. and Walsh, T.R., 2012. First-principles molecular dynamics simulations of NH 4+ and CH3COO− adsorption at the aqueous quartz interface. The Journal of Chemical Physics, 137(22): 224702.

Xie, G. et al., 2022. Synthesis of alkyl polyamine with different functional groups and its montmorillonite swelling inhibition mechanism: Experiment and density functional theory simulation. Applied Clay Science, 230: 106715.

Xu, J., Wang, X., Chen, J., Ding, T. and Xue, J., 2023. Inhibition mechanism of cationic polyacrylamide on montmorillonite surface hydration: A molecular dynamics simulation study. Chemical Physics, 567: 111792.

Yazhgur, P., Vierros, S., Hannoy, D., Sammalkorpi, M. and Salonen, A., 2018. Surfactant Interactions and Organization at the Gas–Water Interface (CTAB with Added Salt). Langmuir, 34(5): 1855-1864.

Yue, Y. et al., 2018. Improving wellbore stability of shale by adjusting its wettability. Journal of Petroleum Science and Engineering, 161: 692-702.

Zeynali, M.E., 2012. Mechanical and physico-chemical aspects of wellbore stability during drilling operations. Journal of Petroleum Science and Engineering, 82-83: 120-124.

Zhang, C. et al., 2022. Synthesis of a hydrophobic quaternary ammonium salt as a shale inhibitor for water-based drilling fluids and determination of the inhibition mechanism. Journal of Molecular Liquids, 362: 119474.

Zhong, H., Qiu, Z., Sun, D., Zhang, D. and Huang, W., 2015. Inhibitive properties comparison of different polyetheramines in water-based drilling fluid. Journal of Natural Gas Science and Engineering, 26: 99-107.